

Smad3 Dosage Determines Androgen Responsiveness and Sets the Pace of Postnatal Testis Development

Catherine Itman, Chin Wong, Briony Hunyadi, Matthias Ernst, David A. Jans, and Kate L. Loveland

Departments of Biochemistry and Molecular Biology (C.I., C.W., D.A.J., K.L.L.) and Anatomy and Cell Biology (C.I., B.H., K.L.L.), Monash University, Melbourne 3800, Australia; and Australian Research Council Centre of Excellence in Biotechnology and Development (C.I., C.W., D.A.J., K.L.L.) and Ludwig Institute for Cancer Research (M.E.), Melbourne 3050, Australia

The establishment and maturation of the testicular Sertoli cell population underpins adult male fertility. These events are influenced by hormones and endocrine factors, including FSH, testosterone and activin. Activin A has developmentally regulated effects on Sertoli cells, enhancing proliferation of immature cells and later promoting postmitotic maturation. These differential responses correlate with altered mothers against decapentaplegic (SMAD)-2/3 signaling: immature cells signal via SMAD3, whereas postmitotic cells use both SMAD2 and SMAD3. This study examined the contribution of SMAD3 to postnatal mouse testis development. We show that SMAD3 production and subcellular localization are highly regulated and, through histological and molecular analyses, identify effects of altered *Smad3* dosage on Sertoli and germ cell development. *Smad3*^{+/-} and *Smad3*^{-/-} mice had smaller testes at 7 d postpartum, but this was not sustained into adulthood. Juvenile and adult serum FSH levels were unaffected by genotype. *Smad3*-null mice displayed delayed Sertoli cell maturation and had reduced expression of androgen receptor (AR), androgen-regulated transcripts, and *Smad2*, whereas germ cell and Leydig cell development were essentially normal. This contrasted remarkably with advanced Sertoli and germ cell maturation and increased expression of AR and androgen-regulated transcripts in *Smad3*^{+/-} mice. In addition, SMAD3 was down-regulated during testis development and testosterone up-regulated *Smad2*, but not *Smad3*, in the TM4 Sertoli cell line. Collectively these data reveal that appropriate SMAD3-mediated signaling drives normal Sertoli cell proliferation, androgen responsiveness, and maturation and influences the pace of the first wave of spermatogenesis, providing new clues to causes of altered pubertal development in boys. (*Endocrinology* 152: 2076–2089, 2011)

Testicular Sertoli cells mediate hormone actions to provide the specialized microenvironment essential for spermatogenesis. Appropriate Sertoli cell development and maturation underpin normal adult fertility; hence, identifying how these processes are controlled is relevant to understanding sub- or infertility and disorders of testis development and is particularly relevant to the increasing incidence of testicular dysgenesis (1).

The transition of immature, proliferating Sertoli cells into postmitotic, terminally differentiated cells around puberty delimits the size of the adult Sertoli cell population.

Because each Sertoli cell supports a limited number of spermatids (2), potential sperm output is determined by the extent of immature Sertoli cell proliferation and timing of Sertoli cell maturation. Hallmark features of Sertoli cell maturation that are essential for normal fertility include the development of androgen responsiveness (3), formation of the blood-testis barrier (4) and secretion of products to support postmeiotic germ cell survival and differentiation (5) (reviewed in Ref. 6). FSH, thyroid hormone, testosterone, and TGF β superfamily ligands, including TGF β s and activin, influence immature and terminally

ISSN Print 0013-7227 ISSN Online 1945-7170
Printed in U.S.A.

Copyright © 2011 by The Endocrine Society

doi: 10.1210/en.2010-1453 Received December 20, 2010. Accepted February 14, 2011.

First Published Online March 8, 2011

Abbreviations: AR, Androgen receptor; ARKO, AR knockout; DDX4, DEAD box polypeptide 4; dpp, days postpartum; HPG, hypothalamic-pituitary-gonadal; PCNA, proliferating cell nuclear antigen; qRT-PCR, quantitative RT-PCR; SCARKO, Sertoli cell-selective AR knockout; SCP, synaptonemal complex protein; SMAD, mothers against decapentaplegic.

differentiated Sertoli cell function (7–11). This study identifies a new link between activin A and testosterone in these events.

Rodent models have established that activin A exerts distinct, developmentally regulated effects on Sertoli cell proliferation and maturation. Dose-dependent enhancement of proliferation is reported in immature rat Sertoli cells *in vitro* (10) and in mice *in vivo*; mice with reduced activin bioactivity have fewer Sertoli cells (12, 13), whereas mice lacking inhibin (*Inha*^{-/-}), an activin signaling inhibitor, develop Sertoli cell tumors due to their unrestrained proliferation and failure to mature (14). Activin A enhancement of Sertoli cell proliferation appears limited to their immature phase because it does not induce terminally differentiated Sertoli cells to divide (9). Activin also indirectly enhances immature Sertoli cell proliferation by promoting FSH synthesis at the pituitary (9, 10, 15). Rat organ cultures have identified that this period when activin A and FSH synergistically promote Sertoli cell proliferation (9) correlates with transient up-regulation of the activin receptor *ActRIIA* (16).

Reports of developmentally regulated effects of activin A on Sertoli cell proliferation led us to investigate the mechanism underlying this developmental switch. Binding of activin to cell surface receptors activates intracellular signaling molecules including mothers against decapentaplegic (SMAD) proteins and MAPKs (17). In canonical SMAD-mediated signaling, C-terminally phosphorylated SMAD2 and SMAD3 accumulate in the nucleus and regulate transcription. Acute sensitivity of immature mouse Sertoli cells to activin A corresponds to a divergence from the canonical SMAD signaling pathway: in immature, 6 d postpartum (dpp) Sertoli cells, activin A induces dose-dependent phosphorylation of SMAD2 and SMAD3, yet only SMAD3 accumulates in the nucleus. In contrast, both SMAD2 and SMAD3 accumulate in nuclei of maturing, 15-dpp Sertoli cells (8). This differential SMAD2/3 use corresponded to distinct transcriptional outcomes. Transcripts relating to steroid biosynthesis (*Hsd17β1*, *Hsd17β3*) were selectively and dose-dependently up-regulated by activin in 6-dpp Sertoli cells, whereas two markers of Sertoli cell maturation, *Gja1* and *Serpina5*, were up-regulated in 15-dpp cells. These findings were confirmed *in vivo*; *Gja1* and *Serpina5* levels were reduced in testes of juvenile mice with lower activin bioactivity (*Inhba*^{BK/BK}) but increased in *Inha*^{-/-} testes (8).

Identifying how activin directly and indirectly stimulates Sertoli cell proliferation and establishing how Sertoli cells shift to a mature activin response is important for understanding the complex processes regulating male fertility. A key clue recently came from removal of either one or both copies of *Smad3* from *Inha*^{-/-} mice. Instead of

developing tumors, Sertoli cells in these mice escaped inappropriate proliferative signals of supraphysiological activin and terminally differentiated (18). This identified SMAD3 as the key mediator of activin-induced Sertoli cell proliferation and suggested that the transition from immature, proliferating to postmitotic, terminally differentiating state is associated with down-regulation of SMAD3-mediated signaling.

Adult male *Smad3*-null mice are fertile (19), establishing that SMAD3 is not essential for male fertility. Because no characterization of the developing testis in these mice has been performed, we assessed SMAD3 protein localization in developing and adult mouse testes and compared somatic and germ cell maturation between *Smad3*^{+/+}, *Smad3*^{+/-}, and *Smad3*^{-/-} mice at key stages of testis development. Our phenotypic analysis and *in vitro* approaches examining *Smad3* dosage effects on Sertoli cell responses to activin A and FSH reveal a requirement for threshold levels of SMAD3 for normal juvenile testis growth and dose-dependent effects of *Smad3* on Sertoli and germ cell maturation and uncover a novel link between *Smad3* dose, AR expression, and androgen-mediated transcription of *Smad2*. These data collectively illuminate an activin-androgen axis that directs the pace of testis development. This first study relating SMAD3 levels to the timing of the first wave of spermatogenesis identifies the *Smad3*^{+/-} mouse as a model of peripheral precocious puberty and the *Smad3*^{-/-} mouse as one of delayed Sertoli cell development.

Materials and Methods

Experimental animals and tissues

Wild-type mice [C57Bl/6Asmu × CBA/CahWehiAsmu (F1)] were obtained from Monash University Central Animal Services. Investigations conformed to the National Health and Medical Research Council/Commonwealth Scientific and Industrial Research Organisation/Australian Agricultural Council Code of Practice for the Care and Use of Animals for Experimental Purposes and were approved by the Monash University Standing Committee on Ethics in Animal Experimentation. *Smad3*^{+/-} mice were maintained by heterozygous matings, genotyped as described (19), and housed under conventional conditions approved by the Animal Ethics Committee at the Ludwig Institute for Cancer Research (Melbourne, Australia). Juvenile animals were killed by decapitation and adults by carbon dioxide asphyxiation and cervical dislocation before tissue removal.

Testis and body weights were recorded at 7, 16, and 70–91 dpp. One testis was fixed in Bouin's fixative for 5 h and then dehydrated through a graded ethanol series, embedded in paraffin, and sectioned at approximately 4 μm onto Superfrost Plus II slides (Lomb Scientific, Sydney, Australia). The other testis was snap frozen on dry ice and then stored at -80 C.

Cord diameter measurement and scoring of germ cell differentiation

Hematoxylin and eosin-stained testis sections from four 7-dpp litters were examined using a Leica DMI microscope (Leica Biosystems, Mount Waverley, Victoria, Australia). Images were captured using a Leica DC200 camera (Leica Biosystems) and cord diameters measured using ImageJ software version 1.38x (<http://rsbweb.nih.gov/ij/>). Cords were considered circular if perpendicular diameters were within 98–100% of each other. At least 49 sections were measured per genotype. Germ cell differentiation was determined by nuclear morphology in testis sections from seven 16-dpp litters (20). At least 72 round tubule cross-sections were scored per animal.

Serum FSH measurement

Blood was collected using capillary tubes from decapitated 7-dpp mice or cardiac puncture of anesthetized adult mice. Samples were assayed individually in 20- μ l duplicates in a single assay. Serum FSH levels were determined using RIA reagents provided by Dr. A. Parlow (National Institute of Diabetes and Digestive and Kidney Diseases, National Hormone and Peptide Program, Torrance, CA). Iodination preparation and antiserum used were rFSH I-9 and anti-rFSH-S-11, respectively. Results are expressed in terms of NIDDK mFSH-RP-1. The tracer was iodinated using Iodogen reagent (Sigma, St. Louis, MO) and detected with goat antirabbit IgG (GAR no. 12; Monash University, Melbourne, Australia). The lowest limit of detection was 1.30 ng/ml and the within-assay coefficient of variation was 9.1%.

Immunohistochemistry

Section immunohistochemistry was performed as described (21). Antigen retrieval was achieved using an 800-W microwave oven by heating samples to 90 C in 50 mM glycine (pH 3.5) for 10 min and then cooling for 20 min [to detect SMAD3, proliferating cell nuclear antigen (PCNA), DEAD box polypeptide 4 (DDX4), and synaptonemal complex protein (SCP)-3] or heating in 1 mM EDTA-NaOH (pH 8) for 5 min at 100% and then 20% for 5 min and cooling for 1 h (to detect AR) (22). Anti-SMAD3 (Invitrogen, Carlsbad, CA) was used at 0.5 μ g/ml, anti-PCNA (Dako, Carpinteria, CA) at 0.96 ng/ml, anti-AR (Santa Cruz Biotechnology, Santa Cruz, CA) at 0.2 ng/ml, and anti-SCP3 (Abcam, Cambridge, UK) at 1.25 ng/ml. Bound primary antibodies were detected using biotinylated antirabbit antibody (Chemicon, Temecula, CA) or biotinylated antimouse (Chemicon). Signal was amplified with Vectastain Elite ABC kit reagents (Vector Laboratories, Burlingame, CA) according to the manufacturer's instructions and detected with 3,3'-diaminobenzidine tetrahydrochloride (Dako). Anti-DDX4 (Abcam) was used at 1 ng/ml, detected with alkaline phosphatase-conjugated antirabbit (Sigma) using fuchsin substrate chromogen system (Dako). Nuclei were visualized by Harris hematoxylin counterstaining. Sections were dehydrated in an ethanol series and mounted under DPX (BDH Laboratories, Poole, UK) (SMAD3, AR, SCP3) or mounted directly after detection with GVA (Invitrogen) (PCNA, DDX4). Immunohistochemistry was performed on at least two sections greater than 200 μ m apart from at least three independent animals per genotype per age. For each experiment, determination of non-specific binding of secondary and tertiary reagents consisted of identical treatments with primary antibody omitted.

Primary cell culture and SMAD signaling analysis

Enriched 6-dpp Sertoli cells were prepared, treated, and analyzed as previously described (8). At least four animals were used per genotype with more than 200 cells measured per animal.

Proliferation assay

Cells were cultured for 72 h with 50 ng/ml activin A (R&D Systems, Minneapolis, MN) or 390 mIU FSH (GonalF FSH, Serono, Australia). DNA synthesis was monitored by tritiated thymidine incorporation [(methyl-³H)-thymidine, 5 μ Ci/ml] (Amersham Biosciences, Castle Hill, New South Wales, Australia) during the final 18 h. Cells were harvested on a Packard Migrate 196 cell harvester (Packard Instrument, Meriden, CT). Incorporated radionucleotide was counted using a Packard 1900 TR liquid scintillation counter. Assays were performed in quadruplicate with at least $n = 4$ per genotype.

Western blot

Cell lysate preparation and Western blots were performed as described (23). Anti-SMAD2 and anti-SMAD3 were used at 0.25 μ g/ml, anti- β -tubulin (Sigma) at 30 μ g/ml, anti-DDX4 at 0.05 μ g/ml, anti-PCNA at 0.16 μ g/ml, anti-SCP3 at 0.3 μ g/ml, and anti-AR at 0.2 μ g/ml. Bound primary antibodies were detected using goat-antirabbit Alexa Fluor 680 (Invitrogen) or goat-antimouse IR-800 (Rockland, Gilbertsville, PA) and visualized with the Li-Cor Odyssey (John Morris Scientific, Melbourne, Australia). Negative control blots were performed for every experiment using identical samples without primary antibody to assess background signal.

RNA isolation, cDNA synthesis, and quantitative RT-PCR (qRT-PCR)

RNA was prepared using TRIzol (Invitrogen). Contaminating genomic DNA was eliminated using deoxyribonuclease 1 (Ambion, Austin, TX) per the manufacturer's guidelines. RNA integrity was visualized under UV light after electrophoresis of 1 μ g total RNA in a 1.1% formaldehyde gel. One microgram of total RNA was reverse transcribed using 100 U Superscript III reverse transcriptase (Invitrogen) with 2.5 μ M random hexamer oligonucleotides (Roche, Mannheim, Germany) according to the manufacturer's guidelines. qRT-PCR analysis was performed using the Applied Biosystems 7900HT Fast real-time PCR system (Applied Biosystems, Foster City, CA) using 125 nM each of 2'-deoxyadenosine-5'-triphosphate, 2'-deoxycytidine-5'-triphosphate, 2'-deoxythymidine-5'-triphosphate, and 2'-deoxyguanosine-5'-triphosphate (Bioline, Alexandria, New South Wales, Australia), 2.5 mM MgCl₂ (Sigma-Aldrich), 20 μ g/ml 6-ROX (Invitrogen), 100 nM primers, 1 \times AmpliTaq Gold buffer and 10 U/ml AmpliTaq Gold DNA polymerase (Applied Biosystems) in 8% dimethylsulfoxide (Sigma-Aldrich). Supplemental Table 1 lists primer sequences, accession numbers, and amplicon size. Amplification parameters were 95 C for 10 min, 40 cycles of 95 C (15 sec), 62 C (15 sec), and 72 C (30 sec) using cDNAs diluted 1:80. Standard curves were generated using 7- or 16-dpp *Smad3*^{+/+} mouse testis cDNA diluted 1:20/60/180/540/1620. Data were analyzed using SDS software version 2.3 (Applied Biosystems). Target copy number was determined by the Pfaffl comparative threshold cycle method (Δ CT or $\Delta\Delta$ CT) (24). Product purity was assessed by melting curve analysis between 60 and 95 C and specificity by sequencing the generated product (23). Every primer pair in every experiment was tested without template and with RNA samples that were not reverse transcribed;

in every case, no amplification was detected. Differences in cDNA synthesis efficiency were measured by amplification of spike RNA before cDNA synthesis as described (25).

TM4 cell culture and hormone treatment

TM4 Sertoli-derived cells (26) were maintained as described (8). Crystalline testosterone (Sigma) was dissolved in 100% ethanol to 100 mM and stored in glass vials at -20°C . Seventy percent confluent TM4 cells were serum starved for 2 h and then treated with 100 μM testosterone (27) or ethanol vehicle control for 6.5 h. RNA isolation was performed using TRIzol (Invitrogen) as described above. Three independent experiments were performed.

Statistical analysis

Statistical analysis was performed using GraphPad Prism 5 software (GraphPad Inc., La Jolla, CA). Data were tested for normal distribution using the D'Agostino and Pearson normality test. Normally distributed data were analyzed using the two-tailed unpaired *t* test or one-way ANOVA with Tukey's posttest. Data not normally distributed were analyzed by two-tailed Mann-Whitney or Kruskal-Wallis test with Dunn's posttest. Differences were considered significant if $P < 0.05$.

Results

Dynamic SMAD3 production and localization is evident in mouse testes

Immunohistochemical detection of SMAD3 in mouse testis sections using a previously validated antibody (8) identified highly regulated production and subcellular localization in somatic and germ cells (Fig. 1A–D). SMAD3 localized to nuclei of Sertoli, peritubular myoid, and interstitial cells at birth and was nuclear and cytoplasmic in these cells at 5 and 15 dpp. In adult testes, faint cytoplasmic signal in Sertoli cells contrasted with intense signal in interstitial cells. This description differs from a previous report that SMAD3 is limited to Sertoli cells in the adult mouse testis (28), perhaps reflecting different detection methods used. In germ cells, SMAD3 was notably absent from gonocytes at birth. At 5 dpp, a faint signal was detected in spermatogonia, whereas at 15 dpp, intense signal was visible in the pachytene spermatocyte cytoplasm. Acrosomal staining was evident in spermatids in adult testes. Because specific cell types displayed changes in SMAD3 nuclear localization, we proceeded to analyze testes of *Smad3*^{+/-} and *Smad3*^{-/-} mice (19) to probe the functions of SMAD3 during testis development.

A threshold level of SMAD3 is required for normal juvenile testis growth and Sertoli cell proliferation

Body weight, testis weight, and testis to body weight ratios of 7 dpp, 16 dpp, and adult *Smad3*^{+/+}, *Smad3*^{+/-}, and *Smad3*^{-/-} mice are listed in Supplemental Table 2. Testis weights and testis to body weight ratios of

Smad3^{+/-} and *Smad3*^{-/-} mice were significantly lower than those of *Smad3*^{+/+} littermates at 7 dpp. At 16 dpp, *Smad3*^{-/-} testes were significantly smaller than *Smad3*^{+/-} testes. Because reduced testis size is indicative of impaired Sertoli cell proliferation, we assessed seminiferous cord diameter and Sertoli cell proliferation in testis sections from 7-dpp mice. Cord diameter in *Smad3*^{-/-} mice ($65.09 \pm 0.62 \mu\text{m}$) was significantly reduced compared with *Smad3*^{+/+} ($67.65 \pm 0.41 \mu\text{m}$, $P < 0.01$) and *Smad3*^{+/-} ($66.98 \pm 0.33 \mu\text{m}$, $P < 0.05$) littermates (Fig. 1E), suggestive of fewer Sertoli cells. Proliferating Sertoli cells, identified by immunohistochemical detection of PCNA (29) and distinguished from neighboring spermatogonia by detection of DDX4 (30) (Supplemental Fig. 1) unexpectedly identified that *Smad3*^{-/-} Sertoli cells had a higher proliferative index ($45.44 \pm 0.96\%$) compared with *Smad3*^{+/+} ($39.87 \pm 1.25\%$, $P < 0.01$) and *Smad3*^{+/-} ($36.18 \pm 1.68\%$, $P < 0.01$) cells (Fig. 1F).

Because FSH and activin A each stimulate Sertoli cell proliferation, serum FSH levels and Sertoli cell capacity to respond to FSH and activin were measured. Serum FSH levels did not differ between genotypes in 7-dpp or adult mice (Fig. 1G). The capacity of 6-dpp Sertoli cells to proliferate in response to activin or FSH was measured using an established *in vitro* thymidine incorporation assay (9, 10) with cells cultured for 72 h in the presence of 50 ng/ml activin A or 390 mIU FSH (Fig. 1H). Activin A increased thymidine incorporation approximately 2-fold relative to untreated cells, with no differences measured between genotypes. Unexpectedly, FSH induced a greater than 3-fold increase in thymidine incorporation by *Smad3*^{-/-} Sertoli cells (4.27 ± 2.05) compared with wild-type and heterozygous samples (1.33 ± 0.18 and 1.67 ± 0.86 , respectively; $P < 0.05$). These data indicate that decreased FSH availability or an impaired proliferative response to FSH or activin A is unlikely to be the causative factor of smaller testes in *Smad3*^{+/-} and *Smad3*^{-/-} mice. The finding that *Smad3*^{-/-} Sertoli cells displayed a higher proliferative activity *in vivo* and *in vitro* was intriguing. Because proliferation is a feature of immaturity, we further analyzed the maturational state of Sertoli cells of *Smad3*^{-/-}, *Smad3*^{+/-}, and *Smad3*^{+/+} mice.

Activin A induces SMAD2 nuclear accumulation in immature Sertoli cells when SMAD3 is reduced or absent

Sertoli cells display a fundamental change in activin A responsiveness as they mature; immature (6 dpp) Sertoli cells transduce activin signals via SMAD3, whereas maturing (15 dpp) Sertoli cells respond by nuclear accumulation of SMAD2 and SMAD3 (8). We examined whether SMAD2 could transduce activin signals in immature Ser-

SMAD3 localization in mouse testes

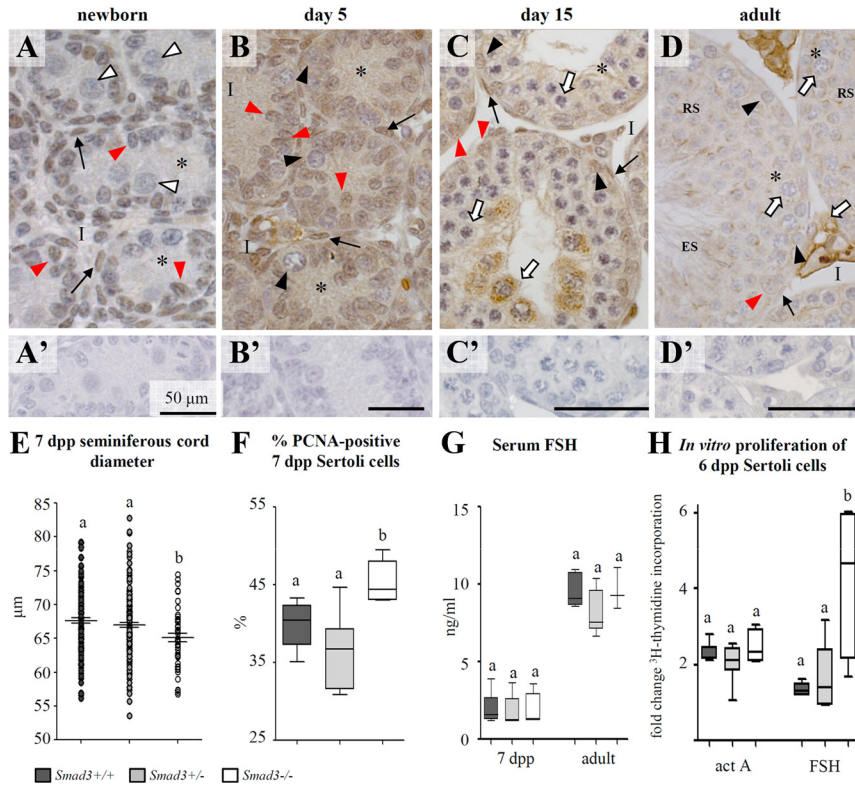


FIG. 1. A–D, Regulated expression and localization of SMAD3 is evident in the immature and adult mouse testis. Localization of SMAD3 by immunohistochemistry (brown staining) in Bouins fixed testis sections from newborn (A), 5 dpp (B), 15 dpp (C), and (D) adult mice. Chromatin is visualized by counterstaining with Harris hematoxylin (blue). No signal was detected when sections were incubated in the absence of primary antibody (A' through D'). White arrowhead, Gonocytes; black arrowhead, spermatogonia; white arrow, spermatocytes; asterisk, Sertoli cell cytoplasm; red arrowhead, Sertoli cell nucleus; black arrow, peritubular cells. RS, Round spermatids; ES, elongating spermatids; I, interstitium. Scale bars, 50 μ m. A, At birth, SMAD3 localized to the nuclei of Sertoli cells, peritubular myoid cells, and interstitial cells but was not detected in gonocytes. B, In the 5-dpp testis, SMAD3 was readily detected in the nuclei and cytoplasm of somatic cells, whereas only a faint cytoplasmic signal was apparent in spermatogonia [as previously described (8)]. C, At 15 dpp, SMAD3 was detected in the nuclei and cytoplasm of Sertoli cells, peritubular myoid cells, and interstitial cells. In germ cells at this age, SMAD3 was readily detected in spermatogonial nuclei and pachytene spermatocyte cytoplasm. D, In the adult testis, faint signal within the seminiferous epithelium was indicative of cytoplasmic localization in Sertoli cells, with acrosomal staining in round and elongating spermatids also apparent. Intense signal was detected in interstitial cells. E–H, *Smad3*-null mice have smaller testis cords and altered Sertoli cell proliferation. Circles (E) represent individual data points, and lines represent mean and SE. Bars (F–H) represent the highest and lowest values measured, boxes indicate the 25th and 75th percentile, and the line indicates the mean. Dark gray, *Smad3*^{+/+}; pale gray, *Smad3*^{+/-}; white, *Smad3*^{-/-}. Significance was determined using the Kruskal-Wallis test and Dunn's posttest with *P* < 0.05 considered significant. Different letters within each age group indicate significant differences. E, Seminiferous cord diameter is significantly smaller in testes of 7-dpp *Smad3*^{-/-} mice (*n* = 7) than in *Smad3*^{+/-} (*n* = 11) and *Smad3*^{+/+} (*n* = 6) littermates (from four litters). A minimum of 49 round cord sections each were measured from each genotype. F, Quantification of PCNA-positive, DDX4-negative cells within the seminiferous epithelium (i.e. Sertoli cells), plotted as percentage. Significantly more Sertoli cells in *Smad3*^{-/-} mice (*n* = 7) were PCNA positive compared with *Smad3*^{+/+} (*n* = 6) and *Smad3*^{+/-} (*n* = 8) littermates. At least 200 Sertoli cells were counted per animal. Representative images of immunohistochemistry and validation of antibody specificity are presented in Supplemental Fig. 1. G, Serum FSH levels in 7-dpp and adult *Smad3*^{+/+}, *Smad3*^{+/-}, and *Smad3*^{-/-} mice, measured by RIA, showed no significant difference between genotypes at either age. 7 dpp, *Smad3*^{+/+} (*n* = 12); *Smad3*^{+/-} (*n* = 15); *Smad3*^{-/-} (*n* = 9). Adult, *Smad3*^{+/+} (*n* = 5); *Smad3*^{+/-} (*n* = 5); *Smad3*^{-/-} (*n* = 3). H, *In vitro* proliferation of 7-dpp Sertoli cells in response to 50 ng/ml activin A or 390 mIU FSH was measured by ³H thymidine incorporation. Graph depicts fold change in thymidine incorporation relative to untreated cells, which was set at 1. All genotypes responded with a 2-fold increase in thymidine uptake relative to untreated cells upon activin A treatment; however, FSH induced significantly a greater proliferative response in Sertoli cells lacking *Smad3*. *Smad3*^{+/+} (*n* = 6); *Smad3*^{+/-} (*n* = 11); *Smad3*^{-/-} (*n* = 4); samples measured in quintuplicate.

toli cells when *Smad3* dosage was reduced. SMAD nuclear accumulation was quantified 45 min after stimulation with 5 ng/ml activin A, a concentration indicated to be physiologically relevant (8). As expected, activin A induced nuclear accumulation of SMAD3 in *Smad3*^{+/+} and *Smad3*^{+/-} Sertoli cells with no signal detected in *Smad3*-null cells (data not shown). Consistent with published data, activin A did not induce SMAD2 nuclear accumulation in *Smad3*^{+/+} cells (2.28 \pm 1.15 vs. 2.26 \pm 0.93, Fig. 2, B and C). However, a 1.19-fold increase in nuclear-localized SMAD2 was measured in *Smad3*^{+/-} cells (2.23 \pm 1.08 vs. 2.65 \pm 1.20, *P* < 0.001) and 1.92-fold increase in *Smad3*-null cells (1.82 \pm 0.66 vs. 3.49 \pm 1.66, *P* < 0.001). Immature *Smad3*^{+/-} and *Smad3*^{-/-} Sertoli cells therefore are activin responsive, with the extent of SMAD2 nuclear accumulation inversely related to *Smad3* dosage.

Nuclear accumulation of both SMAD2 and SMAD3 in activin A-treated 6 dpp *Smad3*^{+/-} Sertoli cells mimics the response observed in 15 dpp, maturing Sertoli cells (8), suggesting their maturation status may be advanced. In contrast, the higher proliferative activity of *Smad3*-null Sertoli cells implied they were less mature. To test these possibilities, we examined the effect of *Smad3* dosage on germ, Sertoli, and Leydig cell development.

The pace of Sertoli cell, but not Leydig cell, maturation depends on *Smad3* dosage

For gene expression analysis by qRT-PCR, *18S*, β *actin*, *ArpboPo*, *Hnrpf*, *Rpl17*, and *Rps21* transcript levels were measured to identify an appropriate standard against which to normalize gene expression between genotypes. No transcript was present at equivalent amounts in total RNA isolated from 7-dpp *Smad3*^{+/+}, *Smad3*^{+/-}, or *Smad3*^{-/-} testes. This was not due to variable efficiency of cDNA synthesis or inconsistent input RNA in cDNA synthe-

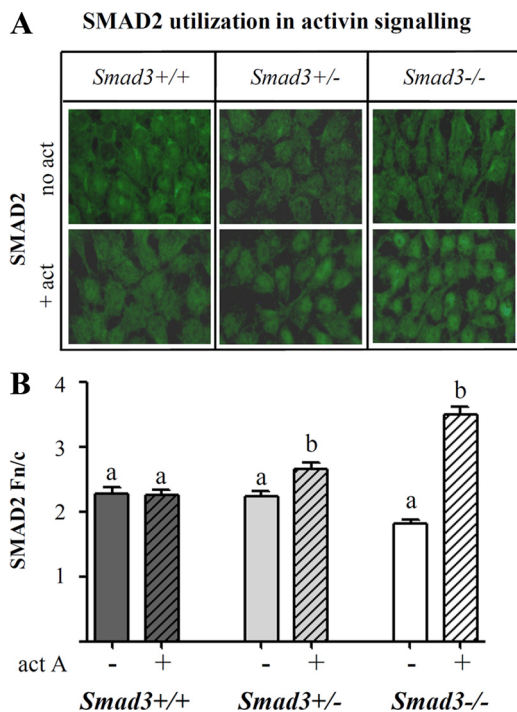


FIG. 2. SMAD2 accumulates in nuclei of activin A-treated *Smad3*^{+/-} and *Smad3*^{-/-} Sertoli cells but not *Smad3*^{+/+} Sertoli cells. A, Use of SMAD2 in activin A (act) signal transduction in Sertoli cells isolated from 7-dpp *Smad3*^{+/+} (n = 5), *Smad3*^{+/-} (n = 4), and *Smad3*^{-/-} (n = 5) mice was assessed by immunofluorescence. No signal was seen in the absence of primary antibody (data not shown). In untreated cells, SMAD2 was similarly distributed in the nucleus and cytoplasm in cells from *Smad3*^{+/+}, *Smad3*^{+/-}, and *Smad3*^{-/-} mice. After 45 min stimulation with 5 ng/ml activin A, no apparent change in SMAD2 localization was observed in Sertoli cells isolated from *Smad3*^{+/+} mice. Some nuclear accumulation of SMAD2 was observed in cells isolated from *Smad3*^{+/-} and obvious nuclear accumulation was observed in cells from *Smad3*^{-/-} mice. B, Quantification of SMAD2 nuclear accumulation in Sertoli cells from A was performed using images captured using a confocal laser-scanning microscope. After activin A (act A) treatment, no nuclear accumulation of SMAD2 was measured in cells isolated from *Smad3*^{+/+} mice (dark gray bars), whereas significant increases were measured in cells from *Smad3*^{+/-} (pale gray bars) and *Smad3*^{-/-} mice (white bars). Hatched bars represent activin A-treated samples. Data are plotted as mean ± SEM, and letters represent significant differences between data sets. Statistical significance was determined using two-tailed Mann-Whitney with Dunn's posttest, with *P* < 0.05 considered significant.

sis reactions (Supplemental Fig. 2). Gene expression was therefore normalized to equivalent quantities of input RNA.

Differences in germ to Sertoli cell ratio between genotypes were assessed by comparing expression of the Sertoli cell marker Wilms tumor homolog 1 (*Wt1*) (31) and the germ cell marker *Ddx4* (30) by qRT-PCR. Expression of these genes was not affected by *Smad3* dosage, determined by measuring transcript levels in isolated Sertoli and germ cells from 7-dpp mice (Fig. 3A). Equivalent ratios of *Ddx4* to *Wt1* in total testes at 7 (Fig. 3B) or 16 dpp (data not shown) indicated no difference in germ to Sertoli cell ratio between genotypes.

Transcripts associated with Sertoli cell maturation that were measured were *anti-Müllerian hormone* (*Amb*)

[down-regulated during maturation (32)] and *Cldn11*, *Tjp1*, *Gja1*, androgen receptor (*Ar*), *Serpina5*, transferrin (*Trf*), *Gata1*, and *p27^{Kip1}* (up-regulated as Sertoli cells mature). *Amb* levels were not different between genotypes at 7 or 16 dpp (Fig. 3, C and D). At 7 dpp, *Cldn11*, *Gja1*, *Serpina5*, and *Trf* transcript levels were significantly reduced in *Smad3*^{-/-} relative to *Smad3*^{+/-} testes, whereas *Ar* and *Gata1* mRNA levels were significantly lower relative to *Smad3*^{+/+} and *Smad3*^{+/-}. *Tjp1* levels were reduced in both *Smad3*^{+/-} and *Smad3*^{-/-} samples relative to the wild type. No difference in *Cdkn1b* transcripts was detected between genotypes at this age. At 16 dpp, *Ar* transcript levels remained significantly lower in *Smad3*^{-/-} compared with *Smad3*^{+/-} testes. *Serpina5* and *Trf* were significantly lower in *Smad3*^{-/-} testes relative to *Smad3*^{+/+} and *Smad3*^{+/-}. More *Cldn11* and *Cdkn1b* transcripts were detected in *Smad3*^{+/-} testes relative to *Smad3*^{+/+} and *Smad3*^{-/-}. Considered together, these data indicate Sertoli cell maturation in *Smad3*^{-/-} mice is delayed at 7 dpp but recovers by 16 dpp. In contrast, maturation of 16-dpp *Smad3*^{+/-} Sertoli cells mice appears relatively advanced.

Leydig cell maturation was examined by measuring expression of genes associated with different stages of development (*Tsp2*, *Cyp11a1*, *Insl3*, *Eh*) and normalized to *Sur2*, which is present at consistent levels throughout Leydig cell development (33). *Sur2* levels were not different between genotypes at 7 or 16 dpp, and we measured no difference in transcript levels of Leydig cell maturation markers (Supplemental Fig. 3).

The first wave of spermatogenesis is advanced in *Smad3*^{+/-} testes

To ascertain the functional relevance of apparent differences in Sertoli cell maturation in *Smad3*^{+/-} and *Smad3*^{-/-} mice, germ cell differentiation was assessed at 7 and 16 dpp. *c-kit* transcripts, found in Leydig cells (34) and differentiating spermatogonia through to pachytene spermatocytes (35–37), were slightly, but significantly, reduced in 7-dpp *Smad3*^{-/-} testes (Fig. 4A). An increased proportion of meiotic germ cells in 7-dpp *Smad3*^{+/-} testes indicated by histological observation was assessed by immunohistochemical detection of the meiotic marker SCP3 (38), confirming *Smad3*^{+/-} mice had a significantly greater proportion of cord sections containing meiotic cells (Figs. 4, B–G).

The most advanced germ cell present in round seminiferous tubule cross-sections at 16 dpp was identified by nuclear morphology (Table 1). Surprisingly, diplotene spermatocytes and round spermatids were present in *Smad3*^{+/-} animals but not in *Smad3*^{+/+} or *Smad3*^{-/-} mice (Fig. 4, H–K). This early appearance of spermatids

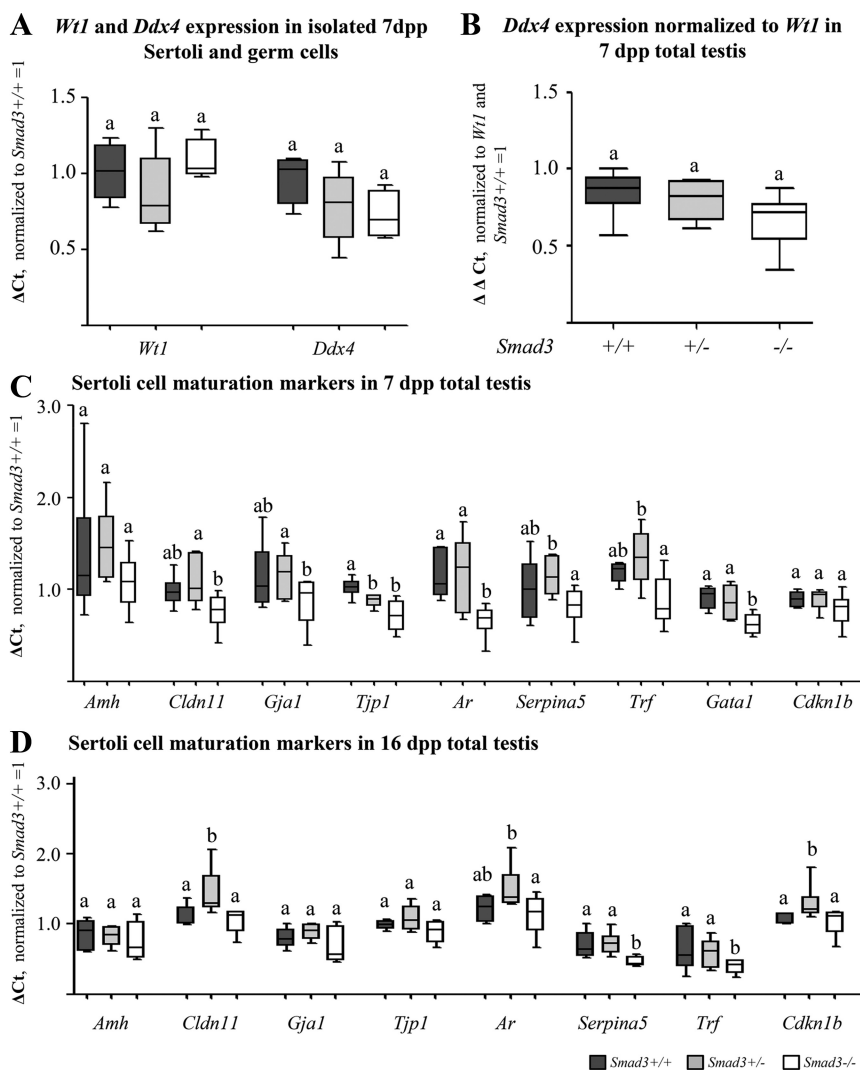


FIG. 3. Transcript analysis indicates Sertoli cell maturation is delayed in *Smad3*^{-/-} mice but advanced in *Smad3*^{+/-} mice. Bars represent the highest and lowest values measured, boxes indicate the 25th and 75th percentiles, and the line indicates the mean. Values were normalized to input RNA and plotted as fold change relative to *Smad3*^{+/+}, which was set at 1. Dark gray, *Smad3*^{+/+}; pale gray, *Smad3*^{+/-}; white, *Smad3*^{-/-}. Significance was determined using two-tailed Mann-Whitney test and Dunn's posttest with $P < 0.05$ considered significant. Different letters within genes measured indicate significant differences. A, Quantitative comparison of *Wt1* and *Ddx4* transcript levels in Sertoli cells and germ cells isolated from 7-dpp *Smad3*^{+/+} ($n = 4$), *Smad3*^{+/-} ($n = 6$), and *Smad3*^{-/-} mice ($n = 4$). No difference in expression of *Wt1* and *Ddx4* was observed between genotypes, indicating that *Wt1* and *Ddx4* expression, and by inference Sertoli and germ cell numbers, is not affected by *Smad3* dosage. B, Quantitative comparison of *Ddx4* mRNA levels plotted relative to *Wt1* mRNAs in total testes of 7-dpp *Smad3*^{+/+} ($n = 6$), *Smad3*^{+/-} ($n = 6$), and *Smad3*^{-/-} ($n = 6$) mice. No difference in *Ddx4*:*Wt1* expression was measured, indicating that the germ cell to Sertoli cell ratio is not affected by *Smad3* dosage. C, Quantitative measurement of transcripts associated with Sertoli cell maturation in testes of 7-dpp *Smad3*^{+/+} ($n = 6$), *Smad3*^{+/-} ($n = 6$), and *Smad3*^{-/-} ($n = 6$) mice. A pattern of significantly lower expression of maturation markers in testes of *Smad3*^{-/-} is suggestive of delayed Sertoli cell maturation relative to *Smad3*^{+/+} and *Smad3*^{+/-} mice. D, Quantitative analysis of transcripts associated with Sertoli cell maturation measured in testes of 16-dpp *Smad3*^{+/+} ($n = 5$), *Smad3*^{+/-} ($n = 8$), and *Smad3*^{-/-} ($n = 5$) mice. Expression of several genes is significantly increased in testes of *Smad3*^{+/-} mice relative to *Smad3*^{+/+} and *Smad3*^{-/-} littermates, indicating that Sertoli cell maturation is advanced in *Smad3*^{+/-} mice at this age.

correlated with increased expression of the spermatid marker *Gapds* (39) in *Smad3*^{+/-} relative to *Smad3*^{-/-} testes (Fig. 4K).

Smad3^{+/+}, *Smad3*^{+/-}, and *Smad3*^{-/-} male mice adults are fertile (19). Histological examination of adult testes revealed no gross difference in spermatogenesis, indicating haploinsufficiency or absence of *Smad3* causes no overt adult spermatogenic phenotype (Fig. 4, L–N).

Smad3 dosage alters Sertoli cell androgen responsiveness

The intriguing finding of reduced *Ar* levels in 7-dpp *Smad3*-null testes led us to examine androgen responsiveness in these samples. Immunohistochemical detection of AR protein revealed staining of similar intensity in peritubular and Sertoli cell nuclei in *Smad3*^{+/+} and *Smad3*^{+/-} mice. In *Smad3*^{-/-} testes, peritubular cell staining was visibly reduced and Sertoli cell signal was faint to undetectable (Fig. 5, A–C). The significance of this was examined further by qRT-PCR measurement of androgen-regulated mRNAs in Sertoli and Leydig cells. Sertoli cell-expressed *Rbox5*, *Spinlw1*, and *Drd4* transcripts were significantly lower in 7-dpp *Smad3*^{-/-} testes relative to *Smad3*^{+/+} and *Smad3*^{+/-} (Fig. 5F). At 16 dpp, *Rbox5* and *Spinlw1* were significantly higher in *Smad3*^{+/-} testes compared with *Smad3*^{-/-} and *Drd4* relative to *Smad3*^{+/+} (Fig. 5G). The Leydig cell androgen-regulated *Cyp17a1* transcript was not different at 7 or 16 dpp (Fig. 5H).

Smad3 is required for normal *Smad2* levels in juvenile Sertoli cells

These data reveal that *Smad3* haploinsufficiency is associated with premature attainment of key developmental milestones in Sertoli and germ cells. We thus hypothesized that SMAD3 is down-regulated as Sertoli cells mature. Consistent with this, Western blot analysis of SMAD proteins in total testis lysates established that SMAD2 protein levels were relatively constant between 4 and 15 dpp and then reduced to approximately half in adult testes. SMAD3 levels rapidly declined around when Sertoli cells cease proliferating (12 dpp), with

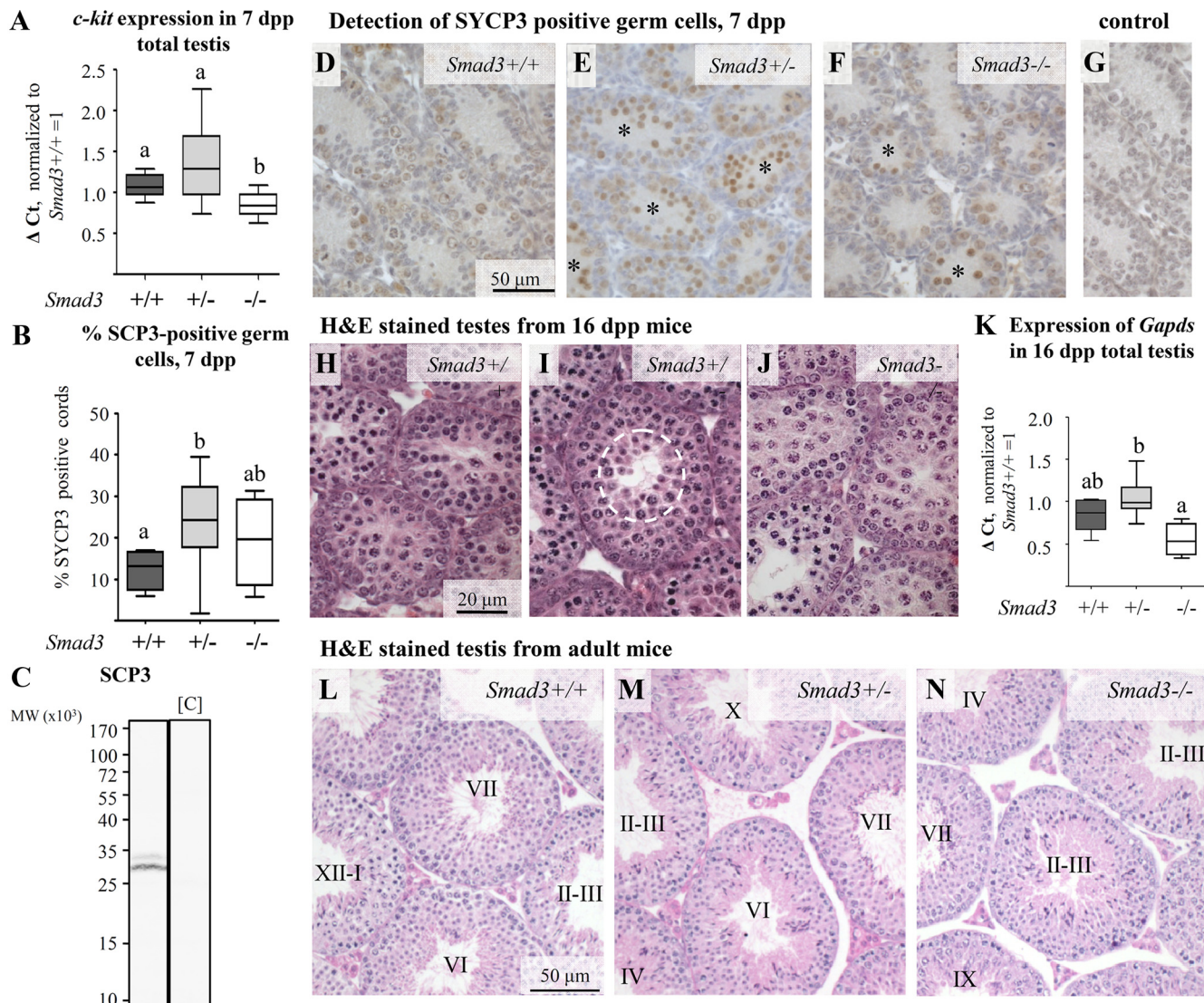


FIG. 4. Spermatogenesis is advanced in *Smad3*^{+/-} mice. Bars represent the highest and lowest values measured, boxes indicate the 25th and 75th percentiles, and the line indicates the mean. Dark gray, *Smad3*^{+/+}; pale gray, *Smad3*^{+/-}; white, *Smad3*^{-/-}. Different letters within genes measured indicate significant differences. A, Quantitative analysis of *c-kit* mRNA levels in testes of 7-dpp *Smad3*^{+/+} (n = 6), *Smad3*^{+/-} (n = 6), and *Smad3*^{-/-} (n = 6) mice identified significantly lower expression in testes from *Smad3*^{-/-} relative to *Smad3*^{+/+} and *Smad3*^{+/-} littermates. Values were normalized to input RNA and plotted as fold change relative to *Smad3*^{+/+}, which was set at 1. *Smad3*^{+/+}, n = 6; *Smad3*^{+/-}, n = 6; *Smad3*^{-/-}, n = 6. Significance was determined using the Kruskal-Wallis test and Dunn's posttest with *P* < 0.05 considered significant. B, Quantification of cord sections containing SCP3-positive spermatocytes established that spermatogenesis in 7-dpp *Smad3*^{+/-} mice was significantly advanced relative to *Smad3*^{+/+} littermates. *Smad3*^{+/+}, n = 4; *Smad3*^{+/-}, n = 8; *Smad3*^{-/-}, n = 8. Significance was determined using one-way ANOVA with Kruskal-Wallis test and Dunn's posttest with *P* < 0.05 considered significant. C, Western blot analysis confirmed that the anti-SCP3 antibody detected bands of the expected size (38) in lysates from the 15-dpp mouse testes with no band observed in the absence [C] of primary antibody. Size markers are indicated to the left. D–G, Representative images of immunohistochemical detection of SCP3 (SYCP3) in testes of 7-dpp *Smad3*^{+/+} (D), *Smad3*^{+/-} (E), and *Smad3*^{-/-} (F) mice identifies early spermatocytes by brown nuclear staining. Sections were counterstained with Harris hematoxylin (blue) for visualization of nuclei. Asterisk, Cord sections containing SCP3-positive spermatocytes. Scale bar, 50 μm. G, No signal was observed within the seminiferous epithelium in the absence of primary antibody. H–J, Visualization of germ cell development in testis sections from 16-dpp *Smad3*^{+/+} (H), *Smad3*^{+/-} (I), and *Smad3*^{-/-} (J) mice by hematoxylin and eosin staining identified the presence of round spermatids in *Smad3*^{+/-} testes only (within dotted white circle) at this age. Bar, 20 μm. K, Expression of *Gapds*, a marker of round spermatids, is significantly greater in testes of 16-dpp *Smad3*^{+/-} mice relative to *Smad3*^{-/-} mice. Values were normalized to input RNA and plotted as fold change relative to *Smad3*^{+/+}, which was set at 1. *Smad3*^{+/+}, n = 5; *Smad3*^{+/-}, n = 8; *Smad3*^{-/-}, n = 5. Significance was determined using the Kruskal-Wallis test and Dunn's posttest with *P* < 0.05 considered significant. L–N, Visualization of stages of spermatogenesis [denoted by Roman numerals (20)] in hematoxylin and eosin-stained testis sections from adult *Smad3*^{+/+} (L), *Smad3*^{+/-} (M), and *Smad3*^{-/-} (N) mice. Bar, 50 μm. No gross difference in testis histology was apparent between genotypes.

a 100-fold lower level measured in adult testes relative to 4 dpp (Fig. 6, A–C). These data also illustrate that SMAD2 and SMAD3 protein are differentially regulated in the testis.

Because use of both SMAD2 and SMAD3 by maturing Sertoli cells in response to activin (8) suggested SMAD2 may be important for Sertoli cell maturation, we measured

TABLE 1. Spermatogenesis is advanced in 16-dpp *Smad3*^{+/-} mice

Genotype	Tubules assessed, n	Preleptotene/leptotene	Zygotene	Pachytene	Diplotene	Round spermatid
<i>Smad3</i> ^{+/+} (n = 3)	503	1.94 ± 1.94% (6)	13.67 ± 4.8% (64)	84.39 ± 6.38% (433)	0 (0)	0 (0)
<i>Smad3</i> ^{+/-} (n = 23)	4531	0.27 ± 0.09% (17)	9.17 ± 0.64% (427)	90.14 ± 0.64% (4072)	0.15 ± 0.09% (7)	0.27 ± 0.1% (8)
<i>Smad3</i> ^{-/-} (n = 6)	732	0.23 ± 0.23% (4)	8.29 ± 1.23% (69)	91.48 ± 1.29% (659)	0 (0)	0 (0)

Data indicate the proportion (*upper value*) and the number (*lower value*) of tubule cross-sections in which the indicated cell type was the most advanced germ cell present. Diplotene spermatocytes and round spermatids were observed only in testes of *Smad3*^{+/-} mice. At least 72 round tubule cross-sections were scored per animal.

Smad2 levels in *Smad3*^{+/+}, *Smad3*^{+/-}, and *Smad3*^{-/-} testes. Remarkably, 7-dpp *Smad3*^{-/-} testes, which have a phenotype of delayed Sertoli cell maturation, have significantly fewer *Smad2* transcripts (0.22-fold reduction, $P < 0.05$). No difference was measured at 16 dpp, when markers of Sertoli cell maturation are equivalent to wild type (Fig. 6C).

Reduced *Smad2* expression in 7-dpp *Smad3*^{-/-} testes with recovery to wild-type levels by 16 dpp is similar to the *Ar* expression profile. We tested whether this reflected a link between androgen and *Smad2* using AR-positive Sertoli-like TM4 cells (26). After 6.5 h stimulation with 100 μ M testosterone or vehicle, *Smad2* and *Smad3* transcript levels were measured by qRT-PCR. Transcript levels were normalized to β -actin, which did not differ between treatments (data not shown). Testosterone selectively increased *Smad2*, but not *Smad3*, relative to controls (Fig. 6D). We therefore speculate that reduced *Smad2* mRNA in 7-dpp *Smad3*^{-/-} testes is a consequence of reduced capacity to respond to testosterone due to lower AR levels.

Discussion

This is the first study to identify that *Smad3* gene dosage affects the pace of testis development. *Smad3* haploinsufficiency is associated with advanced Sertoli cell maturation and spermatogenesis, while the absence of *Smad3* is linked with delayed Sertoli cell maturation. Whereas activin activates several intracellular signaling molecules, including SMAD2, SMAD3, and MAPKs, reducing the availability of just one component of the SMAD-mediated signaling pathway dramatically affects signal transduction and development in the testis.

Our findings converge on current knowledge of androgen actions in the testis. Our identification of an apparent genetic interaction between *Smad3* dosage, AR levels, and *Smad2* is the basis for a model by which the activin-androgen axis programs the pace of testis development (Fig. 7). We propose that a threshold level of SMAD3 in the

immature Sertoli cell is required to ensure normal testis growth and timely AR synthesis. This enables appropriate expression of androgen target genes, including *Smad2*, thereby promoting Sertoli cell maturation. Down-regulation of SMAD3, through as-yet-unknown mechanisms, is associated with cessation of Sertoli cell proliferation and attainment of terminal differentiation. Our model predicts that increased androgen production at puberty would lead to the maintenance, or up-regulation, of SMAD2 in maturing Sertoli cells as SMAD3 levels decline. Correlating with studies showing that altering the SMAD2 to SMAD3 ratio directly influences transcriptional responses to TGF β (40), our data support the hypothesis that shifting the SMAD2 to SMAD3 ratio to favor SMAD2 alters the response of Sertoli cells to activin A as they mature. These data are consistent with our previous finding that the onset of SMAD2 use in activin A signal transduction is associated with Sertoli cell maturation (8).

Interestingly, testis weight and testis to body weight ratios in *Smad3* heterozygous and knockout mice were significantly smaller than those of wild-type littermates at 7 dpp but were equivalent at later ages. We propose that the relatively higher proliferation rate of juvenile *Smad3*^{-/-} Sertoli cells enables testes of these mice to reach wild-type size by 16 dpp, whereas premature appearance of round spermatids in 16 dpp *Smad3*^{+/-} mice increases cell numbers so that testis weights are equivalent to wild type at this age.

Juvenile testis growth reflects the mitogenic actions of activin A and FSH on Sertoli cells (9, 10, 12, 41). Impaired testis growth in juvenile *Smad3*^{+/-} and *Smad3*^{-/-} mice appears independent of serum FSH or Sertoli cell capacity to respond to FSH or activin, suggesting a different mechanism, which we propose to be androgen based. A comparison of mice with constitutive or Sertoli cell-specific AR ablation [AR knockout (ARKO), Sertoli cell-selective AR knockout (SCARKO)] established that androgens indirectly promote Sertoli cell proliferation, likely via peritubular cells (42). We postulate that testes of 7-dpp *Smad3*-

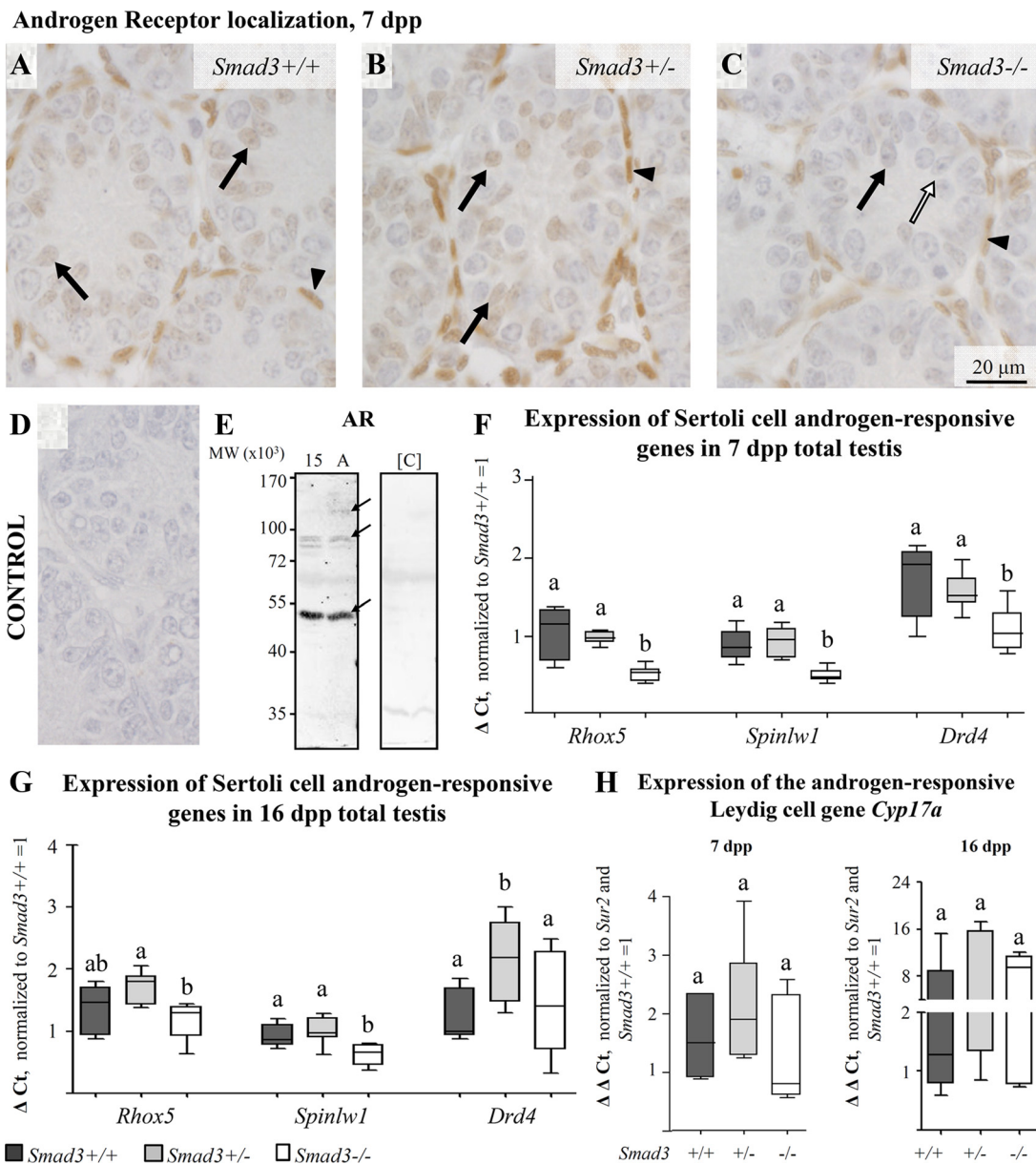


FIG. 5. AR expression and androgen responsiveness is altered in *Smad3*^{+/-} and *Smad3*^{-/-} mice. A–D, Representative images showing immunohistochemical detection of AR in testes from 7-dpp *Smad3*^{+/+} (A), *Smad3*^{+/-} (B), and *Smad3*^{-/-} (C) mice. AR-positive cells are identified by brown nuclear staining. Sections were counterstained with Harris hematoxylin (blue) for visualization of nuclei. Black arrow, AR-positive Sertoli cell nucleus; white arrow, AR-negative Sertoli cell nucleus; black arrowhead, AR-positive peritubular cell. Signals in Sertoli and peritubular cells in *Smad3*^{-/-} testes were consistently less intense than those in sections of *Smad3*^{+/-} and *Smad3*^{+/+} littermates. Scale bar, 20 μm for all images. D, No signal was observed in the absence of primary antibody. E, Western blot analysis shows the anti-AR antibody detected bands of the expected molecular weight of 100, 87, and 50 (arrows) in lysates from 15-dpp (15) and adult (A) mouse testes (60–62), with no band observed in the absence [C] of primary antibody. Size markers are indicated to the left. Bars (F–H) represent the highest and lowest values measured, boxes indicate the 25th and 75th percentiles, and the line indicates the mean. Values were normalized to input RNA and plotted as fold change relative to *Smad3*^{+/+}, which was set at 1. Letters indicate significant differences between data sets. Dark gray, *Smad3*^{+/+}; pale gray, *Smad3*^{+/-}; white, *Smad3*^{-/-}. Significance was determined using Kruskal-Wallis test and Dunn’s posttest with *P* < 0.05 considered significant. F, Expression of the Sertoli cell androgen-regulated genes *Rhox5*, *Spinlw1*, and *Drd4* is significantly reduced in testes of *Smad3*^{+/-} (*n* = 6) mice compared with *Smad3*^{+/+} (*n* = 6) and *Smad3*^{-/-} (*n* = 6) littermates. G, Significantly higher expression of androgen-regulated genes was measured in Sertoli cells of *Smad3*^{+/-} (*n* = 8) mice compared with *Smad3*^{+/+} (*n* = 5) and *Smad3*^{-/-} (*n* = 8) and *Smad3*^{-/-} (*n* = 5) littermates at 16 dpp. H, No difference in transcript levels of the Leydig cell androgen-regulated gene, *Cyp17a*, was observed between genotypes at either 7 dpp (left panel) or 16 dpp (right panel).

null mice are smaller because reduced AR expression impairs the capacity of peritubular cells to indirectly facilitate Sertoli cell proliferation during early testis development. Later, after Sertoli cells become AR positive, androgens act

directly to promote exit from the cell cycle (43). We therefore speculate that delayed onset of AR expression in *Smad3*^{-/-} Sertoli cells impairs their capacity to respond to antiproliferative, maturation-promoting androgen signals.

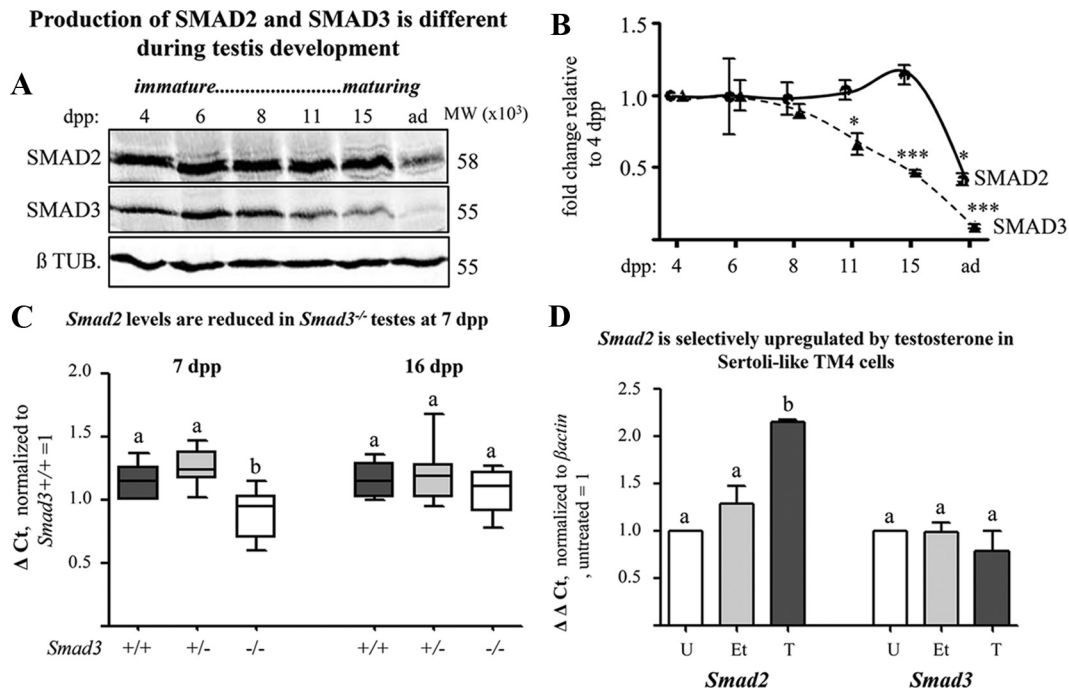


FIG. 6. *Smad2* and *Smad3* mRNA and protein are differentially regulated, with select up-regulation of *Smad2*, but not *Smad3*, by testosterone. **A**, Western blot analysis to detect SMAD2 and SMAD3 using anti-SMAD2 (upper panel) and anti-SMAD3 (middle panel) antibodies identified bands of the expected molecular mass SMAD2 (58 kDa) and SMAD3 (55 kDa) in testis lysates of prepubertal (4–11 dpp), pubertal (15 dpp), and adult mice. Both proteins were detected at each age examined. Detection of β -tubulin (β -TUB; lower panel) served as a loading control. No signal was detected in the absence of primary antibody (data not shown). **B**, Quantification of changes in SMAD2 and SMAD3 protein levels in total testis lysates as presented in **A**, normalized to β -tubulin, from three independent experiments. Data are plotted as mean \pm SEM relative to levels measured in testis lysates of 4-dpp mice, which were set at 1. Significance was determined by using the Kruskal-Wallis test followed by Dunn's posttest; $P < 0.05$ considered significant. *, $P < 0.05$; ***, $P < 0.001$. **C**, Quantitative analysis of *Smad2* transcript levels in testes of 7-dpp *Smad3*^{+/+} ($n = 6$), *Smad3*^{+/-} ($n = 6$), and *Smad3*^{-/-} ($n = 6$) mice identified significantly lower levels in testes from *Smad3*^{-/-} relative to *Smad3*^{+/+} and *Smad3*^{+/-} littermates at 7 dpp but not at 16 dpp. Values were normalized to input RNA and plotted as fold change relative to *Smad3*^{+/+}, which was set at 1. Letters indicate significant difference between data sets. Bars represent the highest and lowest values measured, boxes indicate the 25th and 75th percentile, and the line indicates the mean. Dark gray, *Smad3*^{+/+}; pale gray, *Smad3*^{+/-}; white, *Smad3*^{-/-}. Significance was determined using Kruskal-Wallis test and Dunn's posttest, with $P < 0.05$ considered significant. **D**, Quantitation of *Smad2* and *Smad3* transcript levels in TM4 cells cultured in the presence of 100 μ M testosterone (T; dark gray bars), vehicle control [ethanol (Et); pale gray bars], or medium only [untreated (U); white bars] for 6.5 h ($n = 3$). Testosterone selectively increases *Smad2*, but not *Smad3*, mRNA levels. Transcript measurements were normalized to β -actin, which was stable under all treatments (data not shown). Values are plotted as fold change relative to untreated, which was set at 1. Data are plotted as mean \pm SE with letters indicating significant differences between data sets. Significance was determined by the Kruskal-Wallis test followed by Dunn's posttest, with $P < 0.05$ considered significant.

Additional evidence that the *Smad3*^{+/-} and *Smad3*^{-/-} testicular phenotypes result from altered androgen responsiveness lies in the identification of several essential Sertoli cell transcripts affected by *Smad3* dosage that are androgen regulated. These include protease inhibitors *Serpina5* (44, 45) and *Spinlw1*, the blood-testis barrier component *Cldn11* (44, 46), and cell cycle inhibitor *Cdkn1b* (43), providing the first *in vivo* data showing androgen actions during testis development are modulated by the impact of SMAD3 on AR levels and building on a recent study describing activin/*Smad3*-mediated up-regulation of AR in a prostate cancer cell line (47). Second, we have discovered dose-dependent, nonlinear effects of SMAD3 on AR expression and AR actions *in vivo*: reduced SMAD3 levels are associated with increased AR production and AR target gene expression, yet absence of SMAD3 results in significantly reduced levels of AR and

androgen-regulated transcripts. The testicular phenotypes of *Smad3*^{+/-} and *Smad3*^{-/-} mice are not consistent with altered androgen production because transcript levels of steroidogenic enzymes or the Leydig cell androgen-regulated gene *Cyp17a1* (48) were not different between genotypes. What remains to be established is whether differential expression of androgen target genes in testes of *Smad3*^{+/-} and *Smad3*^{-/-} mice is solely due to differences in AR production or also reflects altered AR activity, perhaps resulting from altered SMAD3-AR interactions, analogous to prostate cancer cell line studies that demonstrate reciprocal effects of SMAD3 on AR transcriptional activity (49).

Comparison of germ cell differentiation in *Smad3*^{+/-} and *Smad3*^{-/-} mice to well-characterized mouse models of altered androgen signaling suggest that Sertoli cells are the primary cell type affected by altered *Smad3* dosage. In

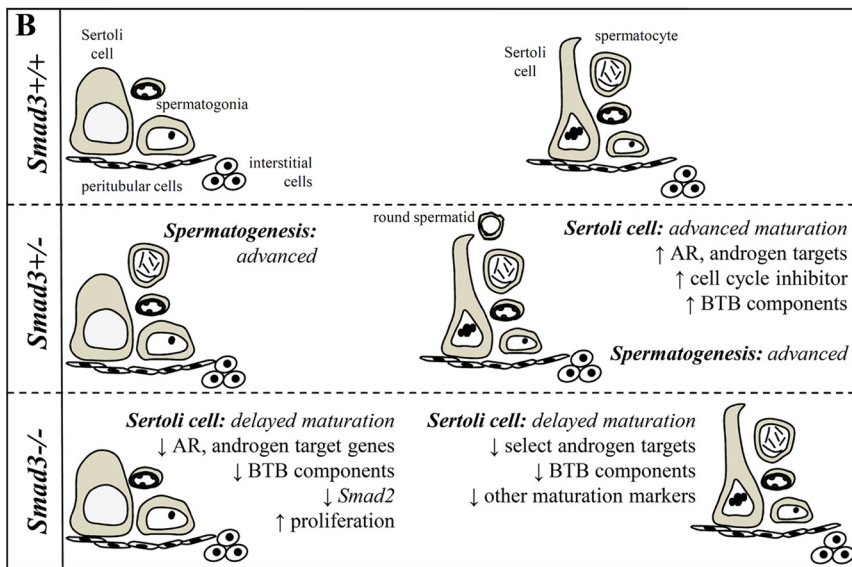
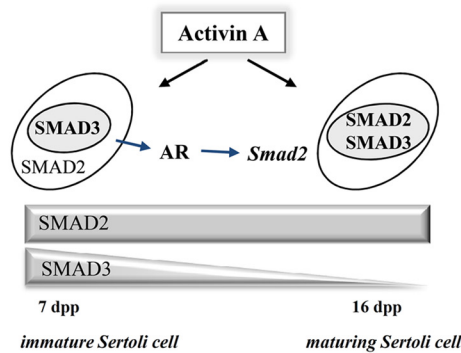
A SMAD3-AR axis defines the pace of normal testicular maturation

FIG. 7. Model depicting the requirement for regulated and interdependent activin and androgen actions for normal testis growth, development, and maturation. A, In the normal immature testis, activin A signals via SMAD3 to promote normal testis growth and steroidogenesis and appropriately timed AR expression. Down-regulation of SMAD3 is associated with the cessation of Sertoli cell proliferation and progression toward a terminally differentiated state. In maturing Sertoli cells, one outcome of AR activation is to up-regulate *Smad2* transcripts. This further promotes Sertoli cell terminal differentiation by contributing to the shift toward use of both SMAD2 and SMAD3 in activin A signal transduction. B, The importance of SMAD3 in directing the normal pace of testis development and maturation is evident in mice that have altered levels of SMAD3. *Smad3* haploinsufficient mice (*Smad3*^{+/-}) display enhanced androgen responsiveness, advanced Sertoli cell maturation, and spermatogenesis, whereas mice that lack *Smad3* (*Smad3*^{-/-}) have impaired androgen responsiveness and delayed Sertoli cell development.

ARKO (50) and SCARKO (50) mice, the *tfm* mouse (51, 52), and the *hpg* mouse (53), spermatogonial differentiation proceeds unaffected through to late pachytene spermatocyte stage, with spermatogenic arrest before completion of meiosis. In the present study, germ cell development in testes of *Smad3*^{-/-} mice during the first wave of spermatogenesis was apparently normal. Furthermore, progression through meiosis during the first wave of spermatogenesis has a higher androgen signaling threshold than does ongoing adult spermatogenesis (54). This provides a plausible explanation of why advanced germ cell differentiation is observed in 16-dpp *Smad3*^{+/-} mice, which display increased testicular expression of *Ar* and androgen-target genes and genes

required to support postmeiotic germ cell survival, all consistent with the measured indicators of increased androgen signaling.

Pubertal development is regulated by the hypothalamic-pituitary-gonadal (HPG) axis and in boys typically occurs between age 8 and 14 yr. Hypothalamic secretion of GnRH stimulates LH and FSH release from the pituitary to act on Leydig and Sertoli cells, respectively (reviewed in Refs. 55 and 56). There is an increasing worldwide recognition of a trend toward precocious puberty (57), which can result from premature activation of the HPG axis (central precocious puberty) or may be HPG independent due to altered testis function (peripheral precocious puberty), such as the presence of Leydig cell tumors (55). Precocious puberty is often associated with elevated androgens (55). We propose that the *Smad3*^{+/-} mouse constitutes a novel model of peripheral precocious puberty in which FSH levels, Leydig cell development, and markers of androgen synthesis are normal. Because androgen effects are mediated by the AR, our findings that *Smad3* dosage influences AR expression in developing Sertoli cells reveals a potentially new etiology of precocious puberty when androgen levels are apparently normal and Leydig cells appear unaffected. On the other hand, endocrine disrupting chemicals are linked to delayed puberty and impaired androgen actions in boys (57, 58). Studies using rats support these human data, with endocrine disruptors exerting broad effects on the developing testis, including changes to Sertoli cell proliferation, maturation, and androgen responsiveness, with the developing testis more sensitive than the adult testis (reviewed in (59)). The *Smad3*^{-/-} mouse phenocopies these human and rodent data, presenting as a model of delayed Sertoli cell development and impaired androgen responsiveness. The *Smad3*^{+/-} and *Smad3*^{-/-} mice therefore offer the opportunity to dissect the control of pubertal development by activin and related signaling molecules and identify SMAD2 and SMAD3 as new targets for reproductive toxicology investigations into altered pubertal development.

Collectively our data demonstrate that normal testis growth and maturation require coordinated and interdependent activin/TGF β and androgen signaling with regulated production of *Smad2*, SMAD3, and AR influencing the balance between cell growth, differentiation, and maturation in establishing the adult testis.

Acknowledgments

We thank Dr. Peter Stanton for the gifts of antiandrogen receptor antibody and testosterone. We also thank Dr. Yuan Zhu and Dr. Jonathan Graff for permission to use the *Smad3*^{-/-} mice, Bianca Teal for excellent management of the *Smad3* mouse colony, Dr. Zhen Zhang for assistance with blood collection, Anne O'Connor and Sue Hayward for performing FSH RIAs, and Dr. Wendy Winnall for spike RNA.

Address all correspondence and requests for reprints to: Associate Professor Kate Loveland, School of Biomedical Sciences, Monash University, Building 77, Level 1, Wellington Road, Clayton, Victoria 3800, Australia. E-mail: kate.loveland@monash.edu.

This work was supported by National Health and Medical Research Council of Australia Grants 545917 and 545916 (to K.L.L.), Grants 487922 and 603122 (to M.E.), Grant APP1002486 (to D.A.J.), Australian Research Council Grants 348239 (to K.L.L.) and 384109 (to D.A.J.), the Operational Infrastructure Support Program by the Victorian Government of Australia (to M.E.), and the Monash University Postgraduate Scholarship and Bridging Postdoctoral Fellowship (to C.I.).

Disclosure Summary: C.I., C.W., B.H., M.E., D.A.J., and K.L.L. have nothing to declare.

References

- Skakkebaek NE, Rajpert-De Meyts E, Main KM 2001 Testicular dysgenesis syndrome: an increasingly common developmental disorder with environmental aspect. *Hum Reprod* 16:972–978
- Orth JM, Gonsalves GL, Lamperti AA 1988 Evidence from Sertoli cell-depleted rats indicates that spermatid number in adults depends on number of Sertoli cells produced during perinatal development. *Endocrinology* 122:787–794
- Wang RS, Yeh S, Tzeng CR, Chang C 2009 Androgen receptor roles in spermatogenesis and fertility: lessons from testicular cell-specific androgen receptor knockout mice. *Endocr Rev* 30:119–132
- Wong CH, Cheng CY 2005 The blood-testis barrier: its biology, regulation and physiological role in spermatogenesis. *Curr Topics Dev Biol* 71:263–296
- Griswold MD 1998 The central role of Sertoli cells in spermatogenesis. *Semin Cell Dev Biol* 9:411–416
- Sharpe RM, McKinnell C, Kivlin C, Fisher JS 2003 Proliferation and functional maturation of Sertoli cells and their relevance to disorders of testis function in adulthood. *Reproduction* 125:769–784
- Holsberger DR, Cooke PS 2005 Understanding the role of thyroid hormone in Sertoli cell development: a mechanistic hypothesis. *Cell Tissue Res* 322:133–140
- Itman C, Small C, Griswold M, Nagaraja AK, Matzuk MM, Brown CW, Jans DA, Loveland KL 2009 Developmentally regulated SMAD2 and SMAD3 utilization directs activin signalling outcomes. *Dev Dyn* 238:1688–1700
- Boitani C, Stefanini M, Fragale A, Morena AR 1995 Activin stimulates Sertoli cell proliferation in a defined period of rat testis development. *Endocrinology* 136:5438–5444
- Buzzard JJ, Farnworth PG, De Kretser DM, O'Connor AE, Wreford NG, Morrison JR 2003 Proliferative phase Sertoli cells display a developmentally regulated response to activin *in vitro*. *Endocrinology* 144:474–483
- Wong EW, Mruk DD, Lee WM, Cheng C 2010 Regulation of blood-testis barrier dynamics by TGF- β 3 is a Cdc42-dependent protein trafficking event. *Proc Natl Acad Sci USA* 107:11399–11404
- Mithraprabhu S, Mendis S, Meachem S, Tubino L, Matzuk MM, Brown CW, Loveland KL 2010 Activin bioactivity affects germ cell differentiation in the postnatal mouse testis *in vivo*. *Biol Reprod* 82:980–990
- Mendis S, Meachem S, Sarraj M, Loveland KL 2010 Activin A balances Sertoli and germ cell proliferation in the fetal mouse testis. *Biol Reprod* 84:379–391
- Matzuk MM, Finegold MJ, Su JG, Hsueh AJ, Bradley A 1992 α -Inhibin is a tumour-suppressor gene with gonadal specificity in mice. *Nature* 360:313–319
- Bilezikjian LM, Blount AL, Donaldson CJ, Vale WW 2006 Pituitary actions of ligands of the TGF- β family: activins and inhibins. *Reproduction* 132:207–215
- Fragale A, Puglisi R, Morena AR, Stefanini M, Boitani C 2001 Age-dependent activin receptor expression pinpoints activin A as a physiological regulator of rat Sertoli cell proliferation. *Mol Hum Reprod* 7:1107–1114
- Shi Y, Massague J 2003 Mechanisms of TGF- β signalling from cell membrane to the nucleus. *Cell* 113:685–700
- Li Q, Graff JM, O'Connor AE, Loveland KL, Matzuk MM 2007 SMAD3 regulates gonadal tumorigenesis. *Mol Endocrinol* 21:2472–2486
- Zhu Y, Richardson JA, Parada LF, Graff JM 1998 *Smad3* mutant mice develop metastatic colorectal cancer. *Cell* 94:703–714
- Russell LD, Ettl RA, Sinha Hikim AD, Clegg EP 1990 Histological and histopathological evaluation of the testis. Clearwater, FL: Cache River Press
- Meehan T, Schlatt S, O'Bryan MK, de Kretser DM, Loveland KL 2000 Regulation of germ cell and Sertoli cell development by activin, follistatin and FSH. *Dev Biol* 220:225–237
- Pileri SA, Roncador G, Ceccarelli C, Piccioli M, Briskomatis A, Sabattini E, Ascani S, Santini D, Piccaluga PP, Leone O, Damiani S, Ercolessi C, Sandri F, Pieri F, Leoncini L, Falini B 1997 Antigen retrieval techniques in immunohistochemistry: comparison of different methods. *J Pathol* 183:116–123
- Itman C, Loveland KL 2008 SMAD expression in the testis: an insight into BMP regulation of spermatogenesis. *Dev Dyn* 237:97–111
- Pfaffl MW 2001 A new mathematical model for relative quantification in real-time RT-PCR. *Nucleic Acids Res* 29:e45
- Craythorn RG, Girling JE, Hedger MP, Rogers PA, Winnall WR 2009 An RNA spiking method demonstrates that 18S rRNA is regulated by progesterone in the mouse uterus. *Mol Hum Reprod* 15:757–761
- Mather JP 1980 Establishment and characterisation of two distinct mouse testicular epithelial cell lines. *Biol Reprod* 23:243–252
- Kaitu'u-Lino T, Sluka P, Foo CFH, Stanton PG 2007 Claudin-11 expression and localization is regulated by androgens in rat Sertoli cells *in vitro*. *Reproduction* 133:1169–1179
- Looyenga BD, Hammer GD 2007 Genetic removal of *Smad3* from inhibin-null mice attenuates tumor progression by uncoupling extracellular mitogenic signals from the cell cycle machinery. *Mol Endocrinol* 21:2440–2457
- Hall PA, Levison DA, Woods AL, Yu CC, Kellock DB, Watkins JA, Barnes DM, Gillett CE, Camplejohn R, Dover R, et al. 1990 Proliferating cell nuclear antigen (PCNA) immunolocalization in paraffin sections: an index of cell proliferation with evidence of deregulated expression in some neoplasms. *J Pathol* 162:285–294

30. Noce T, Okamoto-Ito S, Tsunekawa N 2001 Vasa homolog genes in mammalian germ cell development. *Cell Structure Funct* 26:131–136
31. Pelletier J, Schalling M, Bucker AJ, Rogers A, Haber DA, Housman D 1991 Expression of the Wilms' tumor gene WT1 in the murine urogenital system. *Genes Dev* 5:1345–1356
32. Al-Attar L, Noël K, Dutertre M, Belville C, Forest MG, Burgoyne PS, Josso N, Rey R 1997 Hormonal and cellular regulation of Sertoli cell anti-Mullerian hormone production in the postnatal mouse. *J Clin Invest* 100:1335–1343
33. O'Shaughnessy PJ, Willerton L, Baker PJ 2002 Changes in Leydig cell gene expression during development in the mouse. *Biol Reprod* 66:966–975
34. Yoshinaga K, Nishikawa S, Ogawa M, Hayashi S, Kunisada T, Fujimoto T, Nishikawa S 1991 Role of c-kit in mouse spermatogenesis: identification of spermatogonia as a specific site of c-kit expression and function. *Development* 113:689–699
35. Sandlow JJ, Feng HL, Zheng LJ, Sandra A 1999 Migration and ultrastructural localization of the c-kit receptor protein in spermatogenic cells and spermatozoa of the mouse. *J Urol* 161:1676–1680
36. Ohta H, Tohda A, Nishimune Y 2003 Proliferation and differentiation of spermatogonial stem cells in the *w/w^v* mutant mouse testis. *Biol Reprod* 69:1815–1821
37. Sorrentino V, Giorgi M, Geremia R, Besmer P, Rossi P 1991 Expression of the c-kit proto-oncogene in the murine male germ cells. *Oncogene* 6:149–151
38. Lammers JH, Offenberg HH, van Aalderen M, Vink AC, Dietrich AJ, Heyting C 1994 The gene encoding a major component of the lateral elements of synaptonemal complexes of the rat is related to X-linked lymphocyte-regulated genes. *Mol Cell Biol* 14:1137–1146
39. Welch JE, Schatte EC, O'Brien DA, Eddy EM 1992 Expression of a glyceraldehyde 3-phosphate dehydrogenase gene specific to mouse spermatogenic cells. *Biol Reprod* 46:869–878
40. Kim SG, Kim HA, Jong HS, Park JH, Kim NK, Hong SH, Kim TY, Bang YJ 2005 The endogenous ratio of Smad2 and Smad3 influences the cytoskeletal function of Smad3. *Mol Biol Cell* 16:4672–4683
41. Holsberger DR, Buchhold GM, Leal MC, Kiesewetter SE, O'Brien DA, Hess RA, França LR, Kiyokawa H, Cooke PS 2005 Cell-cycle inhibitors p27Kip1 and p21Cip1 regulate murine Sertoli cell proliferation. *Biol Reprod* 72:1429–1436
42. Tan KA, De Gendt K, Atanassova N, Walker M, Sharpe RM, Saunders PT, Denolet E, Verhoeven G 2005 The role of androgens in Sertoli cell proliferation and functional maturation: studies in mice with total or Sertoli cell-selective ablation of the androgen receptor. *Endocrinology* 146:2674–2683
43. Buzzard JJ, Wreford NG, Morrison JR 2003 Thyroid hormone, retinoic acid and testosterone suppress proliferation and induce markers of differentiation in cultured rat Sertoli cells. *Endocrinology* 144:3722–3731
44. Denolet E, De Gendt K, Allemeersch J, Engelen K, Marchal K, Van Hummelen P, Tan KA, Sharpe RM, Saunders PT, Swinnen JV, Verhoeven G 2006 The effect of a Sertoli cell-selective knockout of the androgen receptor on testicular gene expression in prepubertal mice. *Mol Endocrinol* 20:321–334
45. Willems A, De Gendt K, Allemeersch J, Smith LB, Welsh M, Swinnen JV, Verhoeven G 2010 Early effects of Sertoli cell-selective androgen receptor ablation on testicular gene expression. *Int J Androl* 33:507–517
46. Wang RS, Yeh S, Chen LM, Lin HY, Zhang C, Ni J, Wu CC, di Sant'Agnes PA, deMesy-Bentley KL, Tzeng CR, Cheng C 2006 Androgen receptor in Sertoli cell is essential for germ cell nursery and junctional complex formation in mouse testes. *Endocrinology* 147:5624–5633
47. Kang HY, Huang HY, Hsieh CY, Li CF, Shyr CR, Tsai MY, Chang C, Chuang YC, Huang KE 2009 Activin A enhances prostate cancer cell migration through activation of androgen receptor and is over-expressed in metastatic prostate cancer. *J Bone Miner Res* 24:1180–1193
48. Zhou Q, Shima JE, Nie R, Friel PJ, Griswold MD 2005 Androgen-regulated transcripts in the neonatal mouse testis as determined through microarray analysis. *Biol Reprod* 72:1010–1019
49. Hayes SA, Zarnegar M, Sharma M, Yang F, Peehl DM, ten Dijke P, Sun Z 2001 Smad3 represses androgen receptor-mediated transcription. *Cancer Res* 61:2112–2118
50. De Gendt K, Swinnen JV, Saunders PT, Schoonjans L, Dewerchin M, Devos A, Tan K, Atanassova N, Claessens F, Lécureuil C, Heyns W, Carmeliet P, Guillouf F, Sharpe RM, Verhoeven G 2004 A Sertoli cell-selective knockout of the androgen receptor causes spermatogenic arrest in meiosis. *Proc Natl Acad Sci USA* 101:1327–1332
51. Lyon MF, Glenister PH, Lamoreux ML 1975 Normal spermatozoa from androgen-resistant germ cells of chimeric mice and the role of androgen in spermatogenesis. *Nature* 258:620–622
52. Gaspar ML, Meo T, Bourgarel P, Guenet JL, Tosi M 1991 A single base deletion in the Tfm androgen receptor gene creates a short-lived messenger RNA that directs internal translation initiation. *Proc Natl Acad Sci USA* 88:8606–8610
53. Myers M, Ebling FJ, Nwagwu M, Boulton R, Wadhwa K, Stewart J, Kerr JB 2005 Atypical development of Sertoli cells and impairment of spermatogenesis in the hypogonadal (hpg) mouse. *J Anat* 207:797–811
54. Handelsman DJ, Spaliviero JA, Simpson JM, Allan CM, Singh J 1999 Spermatogenesis without gonadotropins: maintenance has a lower testosterone threshold than initiation. *Endocrinology* 140:3938–3946
55. Carel JC, Léger J 2008 Precocious puberty. *N Engl J Med* 358:2366–2377
56. Brown JJ, Warne GL 2006 Growth in precocious puberty. *Indian J Pediatr* 73:81–88
57. Schoeters G, Den Hond E, Dhooge W, van Larebeke N, Leijts M 2008 Endocrine disruptors and abnormalities of pubertal development. *Basic Clin Pharmacol Toxicol* 102:168–175
58. Den Hond E, Schoeters G 2006 Endocrine disruptors and human puberty. *Int J Androl* 29:264–271; discussion 286–290
59. 2008 Phthalates and cumulative risk assessment: the task ahead. Washington, DC: National Academies Press
60. Wilson CM, McPhaul MJ 1994 A and B forms of the androgen receptor are present in human genital skin fibroblasts. *Proc Natl Acad Sci USA* 91:1234–1238
61. Brinkmann AO, Kuiper GG, Bolt-de Vries J, Mulder E 1988 *In situ* photolabelling of the human androgen receptor. *J Steroid Biochem* 30:257–261
62. Pelley RP, Chinnakannu K, Murthy S, Strickland FM, Menon M, Dou QP, Barrack ER, Reddy GP 2006 Calmodulin-androgen receptor (AR) interaction: calcium-dependent, calpain-mediated breakdown of AR in LNCaP prostate cancer cells. *Cancer Res* 66:11754–11762